T cells genetically engineered to overcome death signaling enhance adoptive cancer immunotherapy

Tori N. Yamamoto,[1,2,3] Ping-Hsien Lee,[1,2] Suman K. Vodnala,[1,2] Devikala Gurusamy,[1,2] Rigel J. Kishton,[1,2] Zhiya Yu,[1,2] Arash Eidizadeh,[1,2] Robert Eil,[4] Jessica Fioravanti,[5] Luca Gattinoni,[5] James N. Kochenderfer,[5] Terry J. Fry,[6] Bulent Arman Aksoy,[7] Jeffrey E. Hammerbacher,[7] Anthony C. Cruz,[8] Richard M. Siegel,[8] Nicholas P. Restifo,[1,2,3] and Christopher A. Klebanoff[9,10,11]

[1]Center for Cancer Research and [2]Center for Cell-Based Therapy, National Cancer Institute (NCI), NIH, Bethesda, Maryland, USA. [3]Immunology Graduate Group, University of Pennsylvania, Philadelphia, Pennsylvania, USA. [4]Memorial Sloan Kettering Cancer Center (MSKCC), New York, New York, USA. [5]Experimental Transplantation and Immunology Branch, NCI, NIH, Bethesda, Maryland, USA. [6]Children's Hospital Colorado, University of Colorado Denver, Aurora, Colorado, USA. [7]Department of Microbiology and Immunology, Medical University of South Carolina, Charleston, South Carolina, USA. [8]National Institute of Arthritis and Musculoskeletal and Skin Diseases, NIH, Bethesda, Maryland, USA. [9]Parker Institute for Cancer Immunotherapy, New York, New York, USA. [10]Center for Cell Engineering and Department of Medicine, MSKCC, New York, New York, USA. [11]Weill Cornell Medical College, New York, New York, USA.

Across clinical trials, T cell expansion and persistence following adoptive cell transfer (ACT) have correlated with superior patient outcomes. Herein, we undertook a pan-cancer analysis to identify actionable ligand-receptor pairs capable of compromising T cell durability following ACT. We discovered that *FASLG*, the gene encoding the apoptosis-inducing ligand FasL, is overexpressed within the majority of human tumor microenvironments (TMEs). Further, we uncovered that Fas, the receptor for FasL, is highly expressed on patient-derived T cells used for clinical ACT. We hypothesized that a cognate Fas-FasL interaction within the TME might limit both T cell persistence and antitumor efficacy. We discovered that genetic engineering of Fas variants impaired in the ability to bind FADD functioned as dominant negative receptors (DNRs), preventing FasL-induced apoptosis in Fas-competent T cells. T cells coengineered with a Fas DNR and either a T cell receptor or chimeric antigen receptor exhibited enhanced persistence following ACT, resulting in superior antitumor efficacy against established solid and hematologic cancers. Despite increased longevity, Fas DNR–engineered T cells did not undergo aberrant expansion or mediate autoimmunity. Thus, T cell–intrinsic disruption of Fas signaling through genetic engineering represents a potentially universal strategy to enhance ACT efficacy across a broad range of human malignancies.

Introduction

Adoptive cell transfer (ACT) using genetically engineered T cells has entered the standard of care for patients with refractory B cell malignancies, including pediatric acute lymphoblastic leukemia (ALL) (1) and adult aggressive B cell lymphomas (2, 3). The efficacy of ACT in hematologic lymphoid malignancies has been consistently observed across clinical trials, regardless of institution, gene vector, or cell composition (4–9). However, responses to adoptive immunotherapy in patients with solid malignancies — collectively the leading cause of adult cancer-related deaths (10) — have been comparatively modest (11–15). Additionally, relapse is increasingly being recognized as a major clinical challenge following ACT for hematologic malignancies despite initially high overall response rates (1, 8). New strategies that enhance the potency of transferred T cells without increasing toxicity are therefore urgently needed if cell therapy is to serve a broader role in the treatment of human cancers (16).

▶ Related Commentary: p. 1522

Conflict of interest: CAK, TNY, and NPR have submitted a US provisional patent (application 62/738,317) related to the Fas DNR technology described in this manuscript.

Submitted: April 6, 2018; **Accepted:** January 15, 2019.
Reference information: *J Clin Invest*. 2019;129(4):1551–1565.
https://doi.org/10.1172/JCI121491.

Multiple variables may influence the success or failure of transferred T cells to mediate cancer regression in patients whose tumor cells uniformly express a target antigen (17). These can include the state of T cell differentiation (18) and local immune-suppressive factors present within the tumor-bearing host (19). Despite these complexities, one of the most consistent correlates of response observed in both hematologic (2, 4–6, 8) and solid cancers (11, 15, 20–22) has been the expansion and/or persistence of transferred T cells following infusion. Building upon this observation, we hypothesized that disruption of factors that negatively regulate T cell proliferation and survival might represent potentially actionable pathways to enhance adoptive immunotherapies. Several clinical trials have tested whether cell-extrinsic approaches can improve the persistence of adoptively transferred T cells, including coadministration of an immune checkpoint inhibitor (23, 24). However, these agents may not always efficiently enter the solid tumor microenvironment (25) and can cause nonspecific immune activation resulting in systemic toxicities that do not contribute to efficacy (26). We therefore pursued a cell-intrinsic strategy to enhance the function of tumor-specific T cells, thereby containing the risk of systemic toxicities and taking full advantage of the ability to reliably genetically engineer human T cells for clinical applications.

Using a pan-cancer analysis to identify candidate ligands that might limit the ability of T cells to expand and persist within

the tumor-bearing host, we discovered that the canonical apoptosis-inducing ligand *FASLG* is preferentially expressed in the majority of human tumor microenvironments (TMEs). Further, we found that most therapeutic T cells used for adoptive immunotherapy for both hematologic and solid cancers constitutively express Fas, the cognate receptor for FasL. Based on these findings, we developed a series of Fas dominant negative receptors (DNRs) that function in both primary mouse and human T cells to prevent FasL-induced apoptosis. Adoptively transferred Fas DNR-engineered T cells showed enhanced T cell persistence and antitumor immunity when co-engineered with either a T cell receptor (TCR) or chimeric antigen receptor (CAR) for the treatment of a solid or liquid cancer, respectively. Despite causing enhanced T cell persistence, this approach did not lead to uncontrolled T cell lymphoproliferation or cause off-target autoimmunity. Collectively, these results provide a potentially universal strategy to enhance the durability and survivability of adoptively transferred T cells for the treatment of a wide range of human malignancies following ACT.

Results

Human TMEs overexpress the death-inducing ligand FASLG. Across human ACT clinical trials for both hematologic and solid cancers, in vivo T cell expansion and persistence have positively correlated with clinical responses (4–6, 11, 21). These observations led us to hypothesize that disruption of pathways that impair T cell proliferation and survival might represent exploitable targets for improving outcomes following adoptive transfer. To determine whether ligands that negatively modulate T cell proliferation and survival are enriched within human TMEs, we compared RNA-Seq data using tumor-containing samples from the TCGA database (https://cancergenome.nih.gov/) relative to matched normal tissues of origin. Given recent evidence that tissues adjacent to resected tumors possess an inflamed transcriptomic profile reflective of an intermediate state between transformed and nontransformed tissues (27), we used expression data from the Genotype-Tissue Expression (GTEx) database (28) as a normal control. In total, we analyzed 9330 samples obtained from 26 different cancer types for which an appropriate matched tissue of origin was available (Supplemental Table 1; supplemental material available online with this article; https://doi.org/10.1172/JCI121491DS1). Raw data from each data set were extracted and normalized in an identical fashion using the RNA-Seq by Expectation Maximization (RSEM) method (29).

We discovered that expression of *FASLG*, the gene encoding the canonical inducer of cellular apoptosis FasL (CD178), was overexpressed in the majority of evaluated cancer types relative to normal tissues (Figure 1A). This included both immunotherapy-responsive cancers, such as cutaneous melanoma (SKCM), renal clear cell carcinoma (KIRC), lung adenocarcinoma (LUAD), and gastroesophageal carcinomas (STAD/ESCA); as well as cancers relatively recalcitrant to current immunotherapies, such as breast carcinoma (BRCA), colorectal adenocarcinoma (READ/COAD), glioblastoma multiforme (GBM), ovarian cancer (OV), pancreatic adenocarcinoma (PAAD), and prostate adenocarcinoma (PRAD). In total, we discovered that 73% (19 of 26) of the human tumor types evaluated exhibited significantly higher expression of *FASLG* within the tumor mass relative to normal tissue controls ($P < 0.05$ to $P < 0.001$; Mann-Whitney U test, Bonferroni-corrected). By contrast, only 19% (5 of 26) of cancer types did not exhibit significant differential expression, and a minority (8%; 2 of 26) showed evidence of reduced *FASLG* expression in tumor samples versus normal tissue.

To gain greater insight into the nature of *FASLG* expression within human TMEs, we performed gene set enrichment analysis (GSEA) (30) using genes positively correlated with *FASLG* across all 26 evaluated cancer types (Figure 1B). We found that expression profiles for many immune-related pathways, including NK cell cytotoxicity, antigen processing and presentation, TCR signaling, primary immune deficiency, and apoptosis, were each significantly enriched (nominal $P < 0.001$, FDR $q < 0.001$). Consistent with these findings, examination of the top 200 genes positively correlated with *FASLG* revealed a predominance of markers associated with both lymphocyte activation, such as IFNG, PRF1, 41BB, and ICOS, and immune counterregulation, including PDCD1, LAG3, and IL10RA (Figure 1C and Supplemental Table 2). Taken together, these data indicated that a death-inducing ligand that might compromise T cell survival is significantly overexpressed in the majority of human cancer microenvironments and is highly correlated to expression signatures of immune activation and regulation.

We next sought to determine whether Fas (CD95), the cognate receptor for FasL, is expressed on the surface of T cells used for clinical adoptive immunotherapy. Previously, we and others found that Fas is expressed on all non-naive human T cell subsets from healthy donors (HDs), including central memory (T_{CM}) cells, effector memory (T_{EM}) cells, and effector memory T cells coexpressing CD45RA (T_{EMRA}) (31, 32). With apheresis products used to generate therapeutic T cells for ACT from patients with melanoma or aggressive B cell lymphomas (diffuse large B cell lymphoma [DLBCL]), we analyzed both the distribution of $CD8\alpha^+$ T cell subsets and the frequency of Fas expression on these subsets. Comparison was made with circulating T cells obtained from a group of age-matched HDs. Consistent with previous reports, we found high expression of Fas on the T_{CM}, T_{EM}, and T_{EMRA} subsets (Figure 1, D and E). Additionally, we discovered that the frequency of Fas^- naive $CD8\alpha^+$ T cells (T_N) in cancer patients was significantly lower than found in HDs (Figure 1F). The depletion of T_N cells likely reflected the influence of prior immune-stimulating and lymphodepleting therapies in the cancer patients analyzed (6, 33, 34). Thus, a significant proportion of human T cells used for ACT express a known death receptor whose cognate ligand might be expressed in the TME.

Fas DNRs prevent T cells from undergoing FasL-mediated apoptosis. Our findings indicated that patient-derived T cells used for adoptive immunotherapy are skewed toward Fas-expressing subsets, which are subsequently transferred into *FASLG*-enriched TMEs. Based on these data, we next investigated whether disruption of Fas signaling within adoptively transferred T cells might prevent their apoptosis and improve in vivo persistence. In addition to triggering T cell apoptosis, FasL is also an essential effector molecule for T cell–mediated tumor killing (35). Further, systemic administration of either an anti-FasL antibody or Fas-Fc fusion protein might induce toxicities, including development of a lymphoproliferative syndrome and accumulation of an abnormal population of double-negative (DN) $CD3^+B220^+CD4^-CD8^-TCR\alpha/\beta^+$ lymphocytes (36, 37). For these

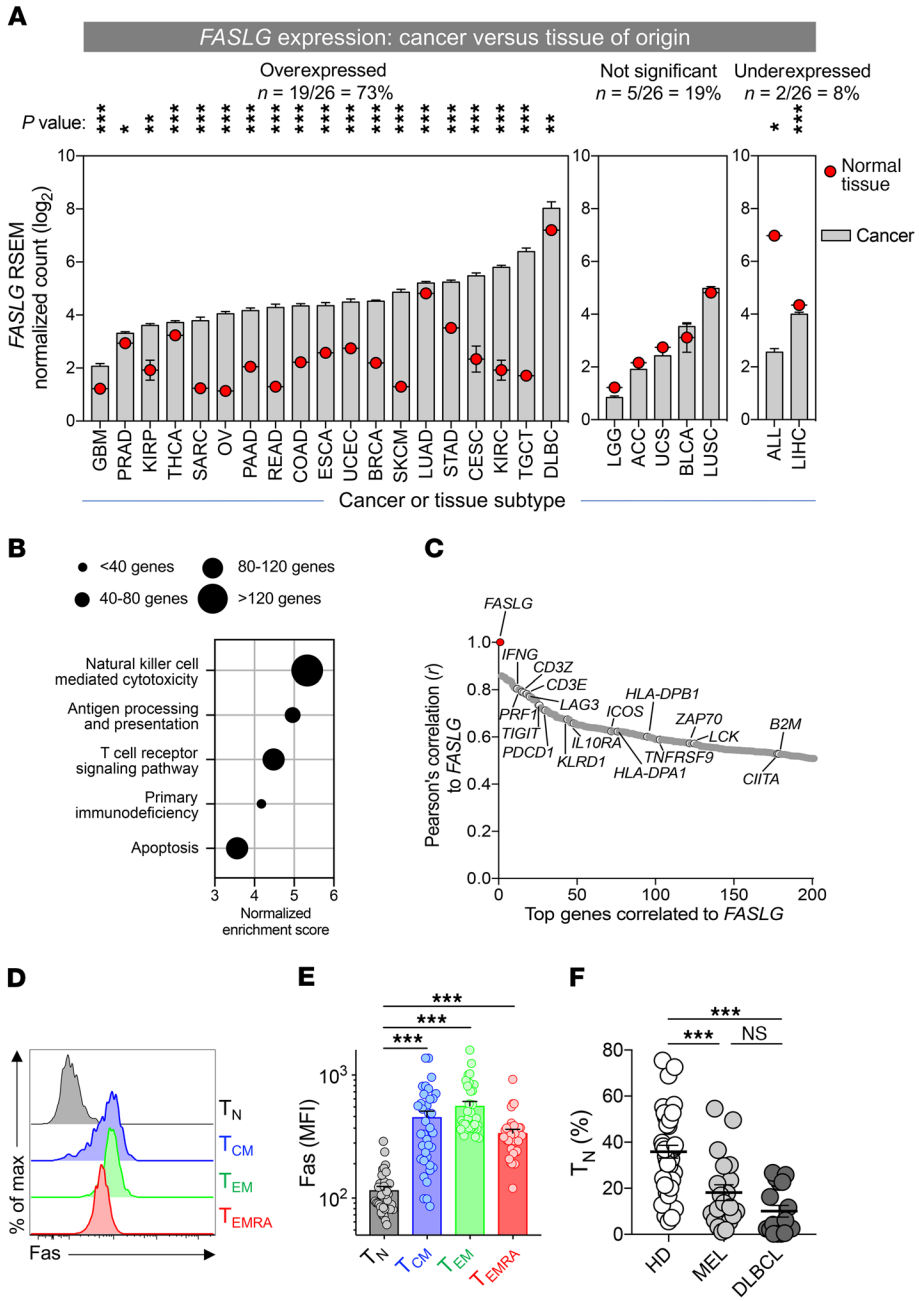

Figure 1. Human TMEs overexpress the death-inducing ligand FASLG. (**A**) A pan-cancer analysis of *FASLG* expression within the microenvironments of 26 different tumor types relative to matched normal tissues of origin. RNA-Seq data from 9330 human cancers and matched normal tissues were extracted from the TCGA and GTEx data sets. Definitions of cancer type abbreviations are shown in Supplemental Table 1. Statistical comparisons of expression between tumors and normal tissues were made using a Mann-Whitney *U* test with Bonferroni's correction; ***$P < 0.001$, **$P < 0.01$, *$P < 0.05$. (**B**) Selected, pre-ranked GSEAs against all KEGG pathways of genes positively correlated to *FASLG* expression averaged across 26 TCGA histologies. Circle diameters reflect the number of genes identified within the GSEA signature sets. The nominal *P* and FDR *q* values for all displayed GSEAs were <0.001. (**C**) Pearson's correlation of the top 200 genes to *FASLG* gene expression across 26 human cancer types in the TCGA database. Selected immune-related genes associated with the GSEA signature sets shown in **B** are identified. *TNFRSF9* is also known as *4-1BB*. Representative histogram (**D**) and summary plot of Fas MFI (**E**) on phenotypically defined CD8α⁺ T cell subsets. Data shown are from peripheral blood T cells from 47 patients and HDs. CD8α⁺ T cell subsets in **D** and **E** were defined as follows: T_N cells, CD8α⁺CD45RA⁺CD45RO⁻CCR7⁺CD62L⁺CD27⁺CD28⁺Fas⁻; T_{CM}, CD8α⁺CD45RO⁺CD45RA⁻CCR7⁺CD62L⁺; T_{EM}, CD8α⁺CD45RO⁺CD45RA⁻CCR7⁻CD62L⁻; T_{EMRA}, CD8α⁺CD45RA⁺CCR7⁻CD62L⁻. ***$P < 0.001$, 1-way ANOVA, corrected with Tukey's multiple comparisons. max, maximum. (**F**) The fraction of T_N among all CD8α⁺ T cells in the circulation of age-matched HDs ($n = 39$; left), and patients with melanoma (MEL; $n = 20$; middle) and DLBCL ($n = 17$; right) at the time of enrollment in an adoptive immunotherapy clinical trial. ***$P < 0.001$, 1-way ANOVA, corrected with Tukey's multiple comparisons.

reasons, we pursued a cell-intrinsic genetic engineering strategy to disable Fas signaling only within tumor-reactive T cells to maintain antitumor potency and minimize the risk of systemic toxicity.

Physiologically, FasL initiates apoptotic signaling by first inducing oligomerization of Fas receptors into trimers or larger oligomers at the cell membrane (Figure 2A) (38). Fas oligomers recruit the intracellular adaptor molecule Fas-associated via death domain (FADD) through homotypic death domains (DDs) present in each molecule (39, 40). Aggregation of FADD recruits the cysteine-aspartic acid protease procaspase-8 (41) through homologous death effector domains in each molecule, forming a death-inducing signaling complex that can initiate the apoptotic signaling cascade (42). Based on this mechanism of action, we hypothesized that overexpression of mutated Fas variants genetically altered to prevent FADD binding would function as DNRs when expressed in Fas-competent WT T cells used for adoptive immunotherapy. Presently, virus-based constructs are the most commonly used methods to stably modify human T cells for clinical application (43). We created a series of retroviral constructs encoding the murine Fas sequence in which either an asparagine residue was substituted for an isoleucine at position 246 of the DD (Fas^{I246N}; a naturally occurring mutant of murine Fas that is unable to bind FADD) (44) or a Fas mutant in which the majority of the intracellular DD was truncated (del aa222–306; $Fas^{\Delta DD}$) to prevent FADD binding (Supplemental Figure 1A and Figure 2A). As controls, we generated both an empty vector construct and a construct encoding the complete WT sequence of Fas (Fas^{WT}). To identify transduced cells, all vectors contained a Thy1.1 reporter separated from Fas using a *Thosea asigna* virus 2A self-cleaving peptide (T2A) sequence.

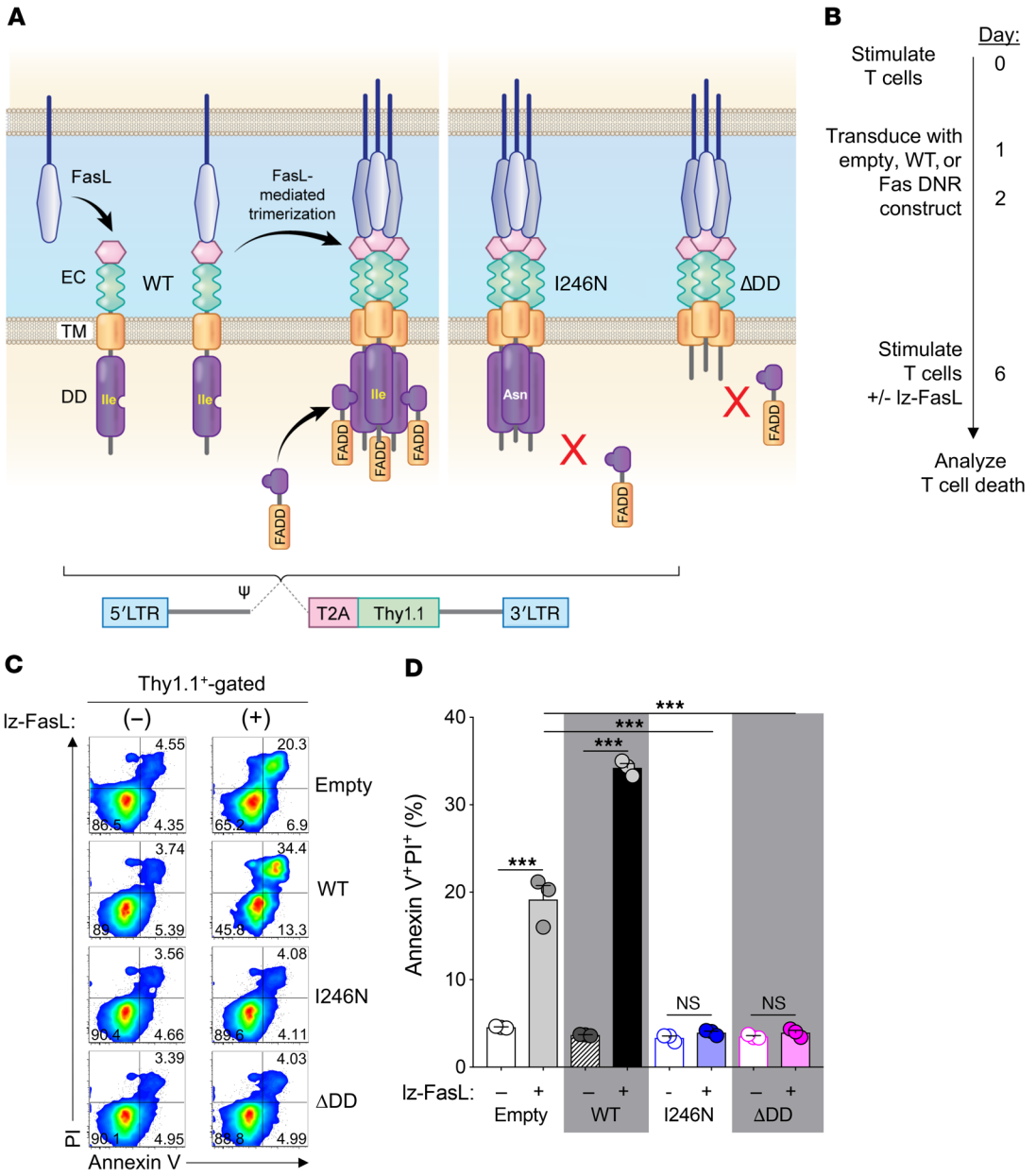

Figure 2. FasL-mediated apoptosis is prevented in T cells engineered with Fas DNRs. (**A**) Schematic representation of physiologic Fas signaling and design of 2 murine Fas DNRs. Fas DNRs were designed to prevent recruitment of FADD by either (i) substitution of an asparagine for an isoleucine residue at position 246 of the DD (Fas^{I246N})or (ii) truncation of the majority of the intracellular DD ($Fas^{\Delta DD}$). WT Fas (Fas^{WT}) and an empty vector were used as controls. Receptors were cloned into a retroviral bicistronic vector containing a Thy1.1 reporter. EC, extracellular domain; TM, transmembrane domain. (**B**) Experimental timeline for the stimulation, retroviral transduction, and testing of Iz-FasL–mediated apoptosis of $CD8\alpha^+$ T cells modified with Fas constructs or an empty vector control. (**C**) Representative FACS plots and (**D**) summary bar graph showing the frequency of apoptotic annexin V^+PI^+ transduced T cells at rest and 6 hours following exposure to Iz-FasL (50 ng ml^{-1}). Results are shown after gating on transduced $Thy1.1^+$ cells. Data are representative of 6 independently performed experiments and displayed as mean ± SEM with $n = 3$ per condition. ***$P < 0.001$, 2-way ANOVA.

T cells were isolated from Fas-competent WT mice; activated by anti-CD3/CD28 antibodies in the presence of IL-2; and transduced with the empty, Fas^{WT}, Fas^{I246N}, or $Fas^{\Delta DD}$ construct (Figure 2B). Phenotypic analysis 6 days following activation and transduction revealed high transduction efficiencies for all constructs as measured by Thy1.1 reporter expression (Supplemental Figure 1, B and C). Notably, ectopic Fas expression was measurably higher than endogenous levels of Fas expression for constructs containing either the WT (6.8-fold higher Fas MFI) or mutant Fas variants (43-fold and 98-fold higher Fas MFI for Fas^{I246N} and $Fas^{\Delta DD}$, respectively; Supplemental Figure 1, B and D).

After 6 days in culture, transduced T cells were stimulated with recombinant FasL molecules oligomerized through a leucine zipper domain (lz-FasL) to mimic the function of membrane-bound FasL (45) or left untreated as controls. In the absence of lz-FasL, T cells transduced with each of the constructs remained similarly

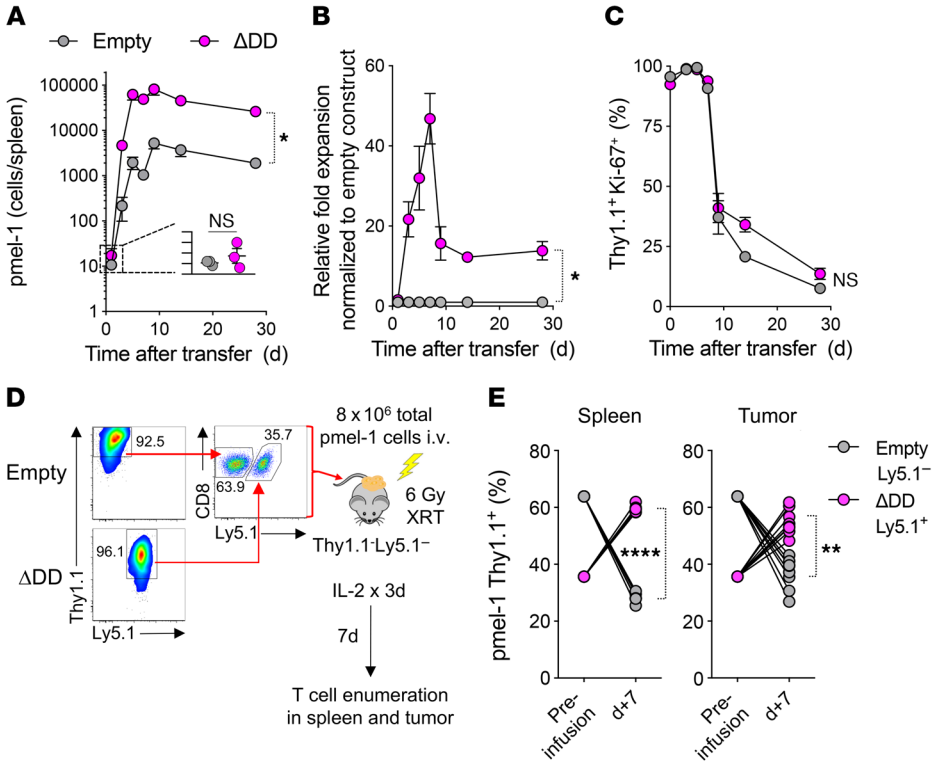

Figure 3. Enhanced persistence and survival of Fas DNR-engineered T cells in vivo. Transduced Ly5.1$^+$ day 11 pmel-1 CD8α$^+$ T cells were generated as described in Figure 2B; then 5 × 10^5 cells from each group were injected into sublethally irradiated (6 Gy) Ly5.2$^+$ B6 mice. Mice were sacrificed on the indicated days and splenocytes analyzed via flow cytometry for homeostatic expansion of Ly5.1$^+$ pmel-1 CD8α$^+$ T cells. (**A**) Total number of live Ly5.1$^+$CD8α$^+$Vβ13$^+$ cells transduced with the empty or Fas$^{\Delta DD}$ construct. (**B**) Relative fold expansion of Fas$^{\Delta DD}$ normalized to empty construct found in spleen on the indicated days. (**C**) Percentage of live Ly5.1$^+$CD8α$^+$ Vβ13$^+$ cells expressing Ki-67 for each condition. Representative plots from 2 independent experiments. Data are displayed as mean ± SEM with n = 3 per condition. *P < 0.05, Wilcoxon's rank-sum test. (**D**) Experimental schema for the generation and co-infusion of pmel-1 T cells engineered with Fas$^{\Delta DD}$ DNR (Ly5.1$^+$Thy1.1$^+$) or an empty vector control (Ly5.1$^-$Thy1.1$^+$). Thy1.1$^+$ T cells were enriched prior to recombination in an approximately 1:1 mixture, and a total of 8 × 10^6 T cells were infused i.v. into sublethally irradiated (6 Gy radiation therapy [XRT]) Thy1.1$^-$Ly5.1$^-$ mice bearing 10-day-established B16 melanoma tumors. Spleens and tumors were harvested for analysis on day 7. (**E**) Relative persistence of Fas$^{\Delta DD}$ DNR–modified to empty vector–modified T cells in the spleens and tumors of recipient mice. Results after gating on live CD8α$^+$Thy1.1$^+$ lymphocytes are representative of 2 independent experiments, each with n = 5–8 mice. "****P < 0.0001, **P < 0.01, paired 2-tailed Student's t test.

viable (Figure 2C). However, following exposure to lz-FasL, a significant proportion of Thy1.1$^+$ T cells transduced with either the empty vector control or Fas^{WT} converted to an apoptotic annexin V$^+$PI$^+$ population (Figure 2, C and D; P < 0.001). Interestingly, overexpression of Fas^{WT} consistently resulted in higher levels of apoptosis relative to those in empty vector–transduced T cells, indicating that expression of Fas above physiologic levels further sensitized T cells to FasL-mediated cell death. By contrast, T cells transduced with either the Fas^{I246N} or Fas$^{\Delta DD}$ vector were almost completely protected from lz-FasL–induced apoptosis. Among pools of T cells transduced with Fas^{I246N} or Fas$^{\Delta DD}$, protection from apoptosis was most evident in the transduced Thy1.1$^+$ populations. However, we also noted a relative increase in the viability of non-transduced Thy1.1$^-$ T cells in cultures containing cells transduced with Fas^{I246N} or Fas$^{\Delta DD}$ (Supplemental Figure 2). This suggested that Fas^{I246N} and Fas$^{\Delta DD}$ may also protect neighboring T cells from apoptosis, likely by functioning as a "sink" for local FasL.

In T cells modified with Fas^{I246N}, we found neither functional nor genetic evidence of reversion to the WT sequence. We measured selective enrichment for T cells modified with Fas^{I246N} compared with Fas^{WT} following serial in vitro restimulations, which indicated that the DNR remained functionally intact over time (Supplemental Figure 3, A and B). Further, Sanger sequencing of serially restimulated, Fas^{I246N}-transduced T cells showed no evidence of reversion of the I246N point mutation to the WT Fas sequence (Supplemental Figure 3, C and D). Thus, overexpression of Fas variants disabled in their ability to bind FADD function in a dominant negative manner to prevent FasL-mediated apoptosis in WT T cells.

Finally, we sought to ascertain whether the Fas DNRs afforded protection from other apoptosis-inducing stimuli that adoptively transferred T cells might encounter in vivo. These include activation-induced cell death (AICD), cytokine withdrawal, and proximity to tumor cells. For these assays, we utilized pmel-1 T cells specific for the cancer antigen gp100 and B16 melanoma engineered to express human gp100 (B16 cells). Although B16 cells did not express FasL at rest, FasL expression was measurably upregulated following incubation with IFN-γ (Supplemental Figure 4). We found that pmel-1 T cells transduced with Fas^{I246N} or Fas$^{\Delta DD}$ were equally protected from apoptosis triggered by either lz-FasL or tumor coculture (Supplemental Figure 5). By contrast, transduction of T cells with Fas$^{\Delta DD}$ resulted in significantly greater cell viability following

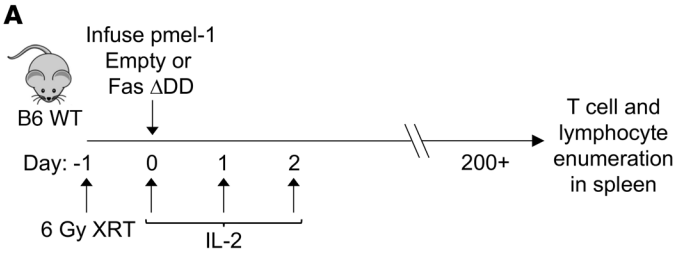

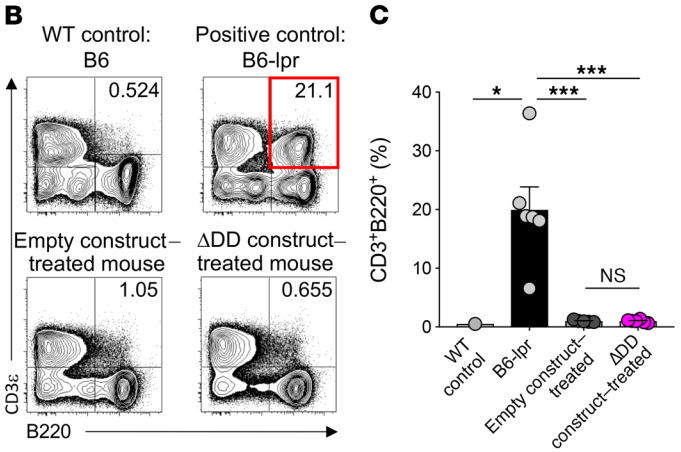

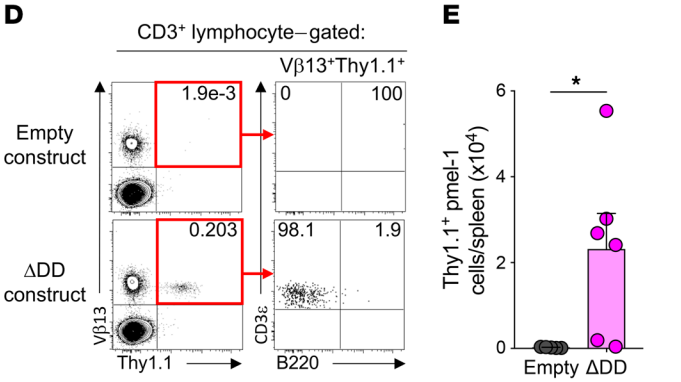

Figure 4. Transfer of Fas DNR–modified T cells does not result in acquired ALPS. (**A**) Experimental design to analyze long-term persistence of WT pmel-1 CD8α+ T cells modified with Fas$^{\Delta DD}$ or empty vector control in B6 mice. (**B**) Representative FACS plots and (**C**) summary bar graph of the frequency of CD3+B220+CD4-CD8α- lymphocytes in the spleens of sublethally irradiated WT mice that received 5 × 10^5 bead-purified Thy1.1+ pmel-1 T cells modified with Fas$^{\Delta DD}$ DNR or an empty vector control. Age-matched WT mice and Fas-deficient B6-lpr mice served as negative and positive controls, respectively. ***P < 0.001, *P < 0.05, 2-way ANOVA. (**D**) Representative FACS plots and (**E**) summary bar graph demonstrating the persistence and surface phenotype of transferred pmel-1 Thy1.1+ T cells modified with Fas$^{\Delta DD}$ DNR or an empty vector control. All data shown are representative of 5 independent experiments, each with n = 5–8 mice per cohort. *P < 0.05, 1-way ANOVA.

AICD induction through anti-CD3/CD28 restimulation or acute cytokine withdrawal relative to cells modified with Fas^{I246N}. These findings were potentially attributable to the ability of the Fas^{I246N} variant to bind to FADD with reduced efficiency under certain conditions (46). We therefore subsequently focused exclusively on the Fas$^{\Delta DD}$ DNR for all in vivo experiments given its superior functional attributes. This permitted us to more clearly determine the influence of removing Fas signaling on the in vivo function of adoptively transferred T cells.

Adoptive transfer of T cells engineered with Fas DNR results in superior persistence. Having established that modification with Fas$^{\Delta DD}$ prevented T cell apoptosis in vitro across a diverse range of apoptosis-inducing stimuli, we sought next to determine whether engineering with this Fas DNR resulted in superior in vivo persistence following adoptive transfer. We therefore adoptively transferred congenically marked, gene-modified pmel-1 T cells into sublethally irradiated Thy1.1$^-$ C57BL/6 (B6) mice to induce homeostatic proliferation, and measured the expansion and persistence of transferred cells over time. T cells transduced with Fas$^{\Delta DD}$ or empty vector control were identified by expression of the Thy1.1 reporter gene. To measure T cell proliferation, we co-stained for the cellular proliferation marker Ki-67.

One day after transfer, we found that Fas$^{\Delta DD}$- and empty vector–modified pmel-1 T cells engrafted at similar levels and almost uniformly expressed Ki-67 (Figure 3, A–C). Beginning within 3 days of transfer, we measured a multi-log expansion of both populations of modified cells. However, at the peak of expansion, we noted an approximately 50-fold greater increase in the numbers of Fas$^{\Delta DD}$-modified T cells relative to control-modified cells. This in turn led to a more than 10-fold-higher level of persistence of Fas DNR–modified T cells on day 30 (Figure 3, A and B). Over time, we measured a comparable reduction in Ki-67 expression on both engineered T cell populations (Figure 3C), which correlated with reconstitution of the host's endogenous T cell compartment. These data suggested that the in vivo proliferation was comparable between the two engineered T cell populations. However, Fas DNR–modified T cells demonstrated superior overall expansion and intermediate-term persistence, likely through a reduction in apoptosis.

We next sought to ascertain whether genetic modification with the Fas DNR resulted in superior T cell persistence within the TME. To ensure that modified T cells were exposed to the same microenvironmental factors within any given tumor, we performed a coinfusion experiment. Congenically distinguishable pmel-1 T cells were obtained from either a Ly5.1$^-$Thy1.1$^-$ or Ly5.1$^+$Thy1.1$^-$ background. Cells were transduced with the Fas$^{\Delta DD}$ DNR or a Thy1.1-expressing empty vector control, respectively. Transduced T cells were subsequently purified using anti-Thy1.1 microbeads, recombined at a roughly 1:1 ratio, then co-infused into sublethally irradiated Ly5.1$^-$Thy1.1$^-$ mice bearing 10-day-established B16 melanoma tumors (Figure 3D). As is currently done in many ACT clinical trials for solid tumors, treated mice received a limited course of IL-2 following transfer (14, 15, 20, 47, 48). Seven days following infusion, both the spleens and tumors of recipient mice were harvested and analyzed for the presence of adoptively transferred, genetically modified Thy1.1$^+$ pmel-1 T cells. We consistently found significant enrichment of Ly5.1$^+$Thy1.1$^+$ Fas$^{\Delta DD}$-modified T cells relative to Ly5.1$^-$Thy1.1$^+$ empty vector–modified T cells in both the spleen and tumor of recipient mice (Figure 3E; P < 0.01, P < 0.0001). Together, these results indicated that genetic engineering with a Fas DNR enhanced T cell persistence in vivo in both the spleen and TME following adoptive cell transfer.

ACT of Fas DNR–modified T cells does not result in an acquired ALPS phenotype. Mice and humans with germline defects in com-

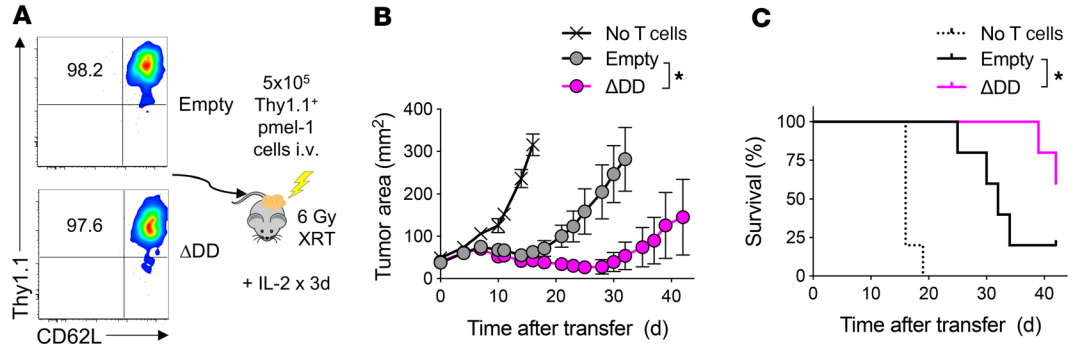

Figure 5. Adoptive transfer of Fas DNR–modified T cells enhances antitumor efficacy independently of T cell differentiation status. (**A**) Representative FACS plots demonstrating the purity of sorted CD62L$^+$CD44$^+$Thy1.1$^+$ T_{CM}-like pmel-1 T cells modified with Fas$^{\Delta DD}$ or empty vector control prior to infusion. The percentage of gated Thy1.1$^+$CD62L$^+$ cells is shown in the FACS plot. (**B**) Tumor regression and (**C**) survival of mice bearing 10-day-established B16 melanoma tumors that were untreated or received 5 × 10^5 of sort-purified T_{CM}-like Thy1.1$^+$ modified cells. Representative results from 2 independent experiments are shown as mean ± SEM using n = 5–8 mice/cohort. Statistical comparisons were performed using Wilcoxon's rank-sum test (**B**) or log-rank Mantel-Cox test (**C**); *P < 0.05.

ponents of apoptotic signaling can develop profound alterations in normal lymphocyte homeostasis and development. These abnormalities, collectively referred to as autoimmune lymphoproliferative syndrome (ALPS), include the accumulation of an aberrant DN lymphocyte population, the development of autoantibodies, and impaired survival (49, 50). Given the potential safety concerns related to disabling normal Fas signaling in mature T cells, we performed long-term immune monitoring of animals that received Fas$^{\Delta DD}$ DNR–modified T cells more than 6 months prior (Figure 4A). This time point was chosen because mice with germline defects in Fas typically develop overt clinical manifestations within the first 3.5–5 months of life, depending on the background strain (51, 52). Using unmanipulated B6 WT and Fas-deficient lpr (B6-lpr) mice as respective negative and positive controls for the ALPS phenotype, we assessed the frequency of CD3$^+$B220$^+$ lymphocytes in the spleens of mice that had previously received ACT of Thy1.1$^+$Vβ13$^+$ pmel-1 T cells modified with the Fas$^{\Delta DD}$ DNR or empty vector control. As expected, the spleens of B6-lpr mice exhibited a significant accumulation of abnormal CD3$^+$B220$^+$ lymphocytes relative to WT controls (Figure 4, B and C; P < 0.05, P < 0.001). By contrast, there was no significant increase in this population in the mice receiving T cells modified with either empty vector or Fas DNR. To exclude the possibility of transformation of the modified T cell population, we assessed the long-term persistence and phenotype of transferred Vβ13$^+$Thy1.1$^+$ engineered T cells. Consistent with our findings at intermediate time points, we found that T cells engineered with Fas$^{\Delta DD}$ DNR persisted at higher numbers than cells modified with the empty vector after more than 200 days (Figure 4, D and E; P < 0.05). Long-term-persisting Fas DNR–modified T cells maintained a conventional CD3$^+$B220$^-$ phenotype. These data indicated that adoptively transferred pmel-1 T cells expressing the Fas DNR did not undergo abnormal lymphoproliferation in B6 hosts.

It was previously shown that expression of a transgenic TCR crossed to a Fas-deficient lpr background can limit the development of ALPS (53). Additionally, the B6 strain manifests lymphoproliferative symptoms at a slower rate compared with other strains (51, 52, 54). We therefore performed additional experiments to assess the safety of the Fas$^{\Delta DD}$ DNR modification by adoptively transferring an open T cell repertoire genetically engineered with either Fas DNR or empty control into the ALPS-susceptible MRL-Mp strain. Fas-deficient mice on an MRL background (MRL-lpr mice) develop autoantibodies, nephritis, and splenomegaly more severely and many months earlier than B6-lpr mice (Supplemental Figure 6A) (51, 52, 54).

To induce activation and expansion of adoptively transferred T cells in this model, we cotransduced open-repertoire T cells from the MRL-Mp mouse with a previously described second-generation anti-CD19 28ζ CAR (55) and the Fas$^{\Delta DD}$ or control vector. Use of the anti-CD19 CAR in these experiments promoted strong in vivo proliferation of T cells through recognition of host CD19$^+$ B cells. Of note, recently published data indicate that T cells modified with a CAR are still able to undergo stimulation through their TCR (56, 57).

We analyzed the spleens of MRL-Mp mice that received no cells (PBS), or anti-CD19 CAR$^+$ T cells transduced with Fas$^{\Delta DD}$ or empty control and compared these with the spleens of age-matched Fas-deficient MRL-lpr mice (Supplemental Figure 6C). We found that spleens from age-matched MRL-lpr mice weighed significantly more when compared with spleens from all other treatment groups. Importantly, we measured no difference in spleen sizes between PBS-treated mice and mice that received anti-CD19 CAR–transduced cells modified either with the Fas$^{\Delta DD}$ or control. Flow cytometry analysis of splenocytes demonstrated a robust expansion of unusual DN CD3$^+$B220$^+$ lymphocytes in the spleens of MLR-lpr mice that collectively accounted for more than 30% of all lymphocytes (Supplemental Figure 6, D and E). By contrast, the frequency of CD3$^+$B220$^+$ lymphocytes in the empty vector and Fas$^{\Delta DD}$ T cell–treated mice was similar to levels observed in the PBS control mice.

To assess for the development of autoimmunity, we performed serum analysis of all treated animals using samples from MRL-lpr mice as a positive control. We found that mice that received anti-CD19 CAR$^+$ T cells modified with Fas$^{\Delta DD}$ or empty vector had low antinuclear and anti-dsDNA antibody titers comparable to the PBS control (Supplemental Figure 6F). In contrast, serum from the MRL-lpr positive control mice demonstrated high titers of both types of autoantibodies.

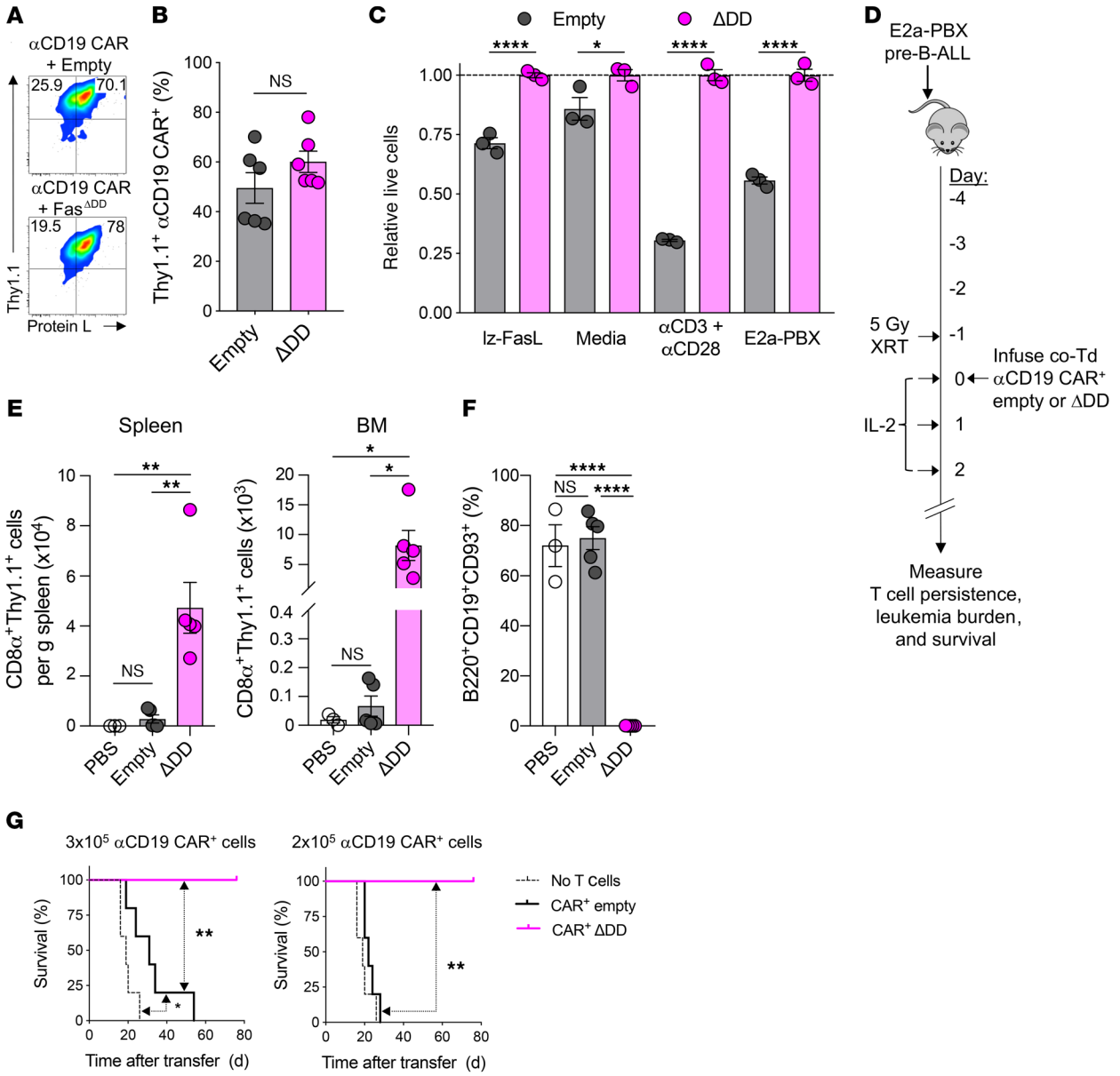

Figure 6. Expression of Fas DNR enhances antiapoptotic functions and in vivo persistence in anti-CD19 CAR model. (**A**) Representative flow plots and (**B**) summary data of double transduction of B6 CD8α+ T cells with retroviral constructs encoding anti-CD19 CAR and empty or Fas DNR. Analysis performed on day 11 after Thy1.1 bead enrichment on day 6. (**C**) Summary bar graph of relative T cell viability (to Fas$^{\Delta DD}$) following overnight culture in cytokine-free media alone, with Iz-FasL (100 ng ml^{-1}), 2 μg ml^{-1} each of anti-CD3 and anti-CD28, or E2a-PBX. Data shown after gating on Thy1.1+ lymphocytes are representative of 3 independently performed experiments, and displayed as mean ± SEM with n = 3 per condition. *P < 0.05, ****P < 0.0001, 2-way ANOVA. (**D**) Experimental schema for the generation and infusion of WT CD8α+ T cells engineered to express anti-CD19 CAR along with Fas$^{\Delta DD}$ DNR or an empty vector control. Transduced T cells were Thy1.1 bead enriched prior to injection, and T cells were infused i.v. into sublethally irradiated (5 Gy) mice bearing 4-day-established E2a-PBX leukemia. Spleens and BM were harvested for analysis on day 14. co-Td, cotransduced. (**E**) Summary data of numbers of live CD8α+Thy1.1+ lymphocytes in spleens and BM of recipient mice. (**F**) Summary data of the frequency of E2a-PBX leukemia in the BM of recipient mice. Results in **E** and **F** are representative of 2 independent experiments, each with n = 3–5 mice. *P < 0.05, **P < 0.01, ****P < 0.0001, 1-way ANOVA, corrected with Tukey's multiple comparisons. (**G**) Survival of mice bearing 4-day-established E2a-PBX leukemia that were untreated or received 3 × 10^5 (left) or 2 × 10^5 (right) anti-CD19 CAR+ Thy1.1+ modified cells. Representative results from 4 independent experiments are shown as mean ± SEM using n = 5 mice/cohort. Statistical comparisons were performed using the log-rank Mantel-Cox test; *P < 0.05 **P < 0.01.

In the absence of uncontrolled lymphoproliferation and the formation of autoantibodies, we found that anti-CD19 CAR+ T cells cotransduced with Fas DNR persisted at significantly higher levels in the spleens of recipient MRL-Mp mice compared with control-modified anti-CD19 CAR+ T cells (Supplemental Figure 6G). Further, the persistent Fas DNR–modified CAR+ T cells did not acquire a greater proportion of aberrant CD3+B220+ cells compared with control-modified CAR+ cells (Supplemental Figure 6H). These results directly mirrored our findings using Fas$^{\Delta DD}$-modified pmel-1 T cells transferred into B6 hosts (Figure 4, D and E).

Finally, to assess whether the ALPS-susceptible MRL-Mp recipient mice developed lung pathology following adoptive transfer

of Fas DNR–modified T cells, we performed a blinded pathologic assessment of H&E-stained lung specimens. Consistent with previous reports (36), we found that the Fas-deficient MRL-lpr mice developed a dense mononuclear cell inflammatory lung infiltrate in the perivascular and peribronchiolar regions (Supplemental Figure 7, A and B). By contrast, mice treated with $Fas^{\Delta DD}$- or control-modified T cells did not display evidence of an increased inflammatory infiltrate relative to PBS-treated control injection. Further, we observed no evidence of pulmonary fibrosis.

Together, these data in both the B6 and MRL-Mp strains demonstrate that despite the augmented survival of the $Fas^{\Delta DD}$ DNR T cells, there was no evidence of uncontrolled lymphoaccumulation, formation of a $Thy1.1^+CD3^+B220^+$ population, or evidence of autoimmunity. Based on these data, we conclude that infusion of mature T cells impaired in Fas signaling does not result in an acquired lymphoproliferative phenotype.

T cell–intrinsic disruption of Fas signaling enhances antitumor efficacy following ACT. Having established that adoptively transferred T cells engineered with a Fas DNR results in enhanced persistence without long-term toxicity, we next evaluated the antitumor efficacy of these cells. We recently discovered that Fas stimulation can induce non-apoptotic Akt/mTOR signaling, resulting in augmented T cell differentiation (58–60). Consistent with our previous results, we found that exposure to lz-FasL caused a dose-dependent increase in phosphorylated Akt^{S473} ($pAkt^{S473}$) and $pS6^{S235,S236}$ in T cells transduced with an empty vector control (Supplemental Figure 8, A and B). Expansion of control-modified cells resulted in an accumulation of T_{EM}-like cells with a reduced capacity to produce IL-2 (Supplemental Figure 8, C and D). By contrast, T cells transduced with a Fas DNR did not increase Akt or S6 phosphorylation following lz-FasL stimulation and were protected from augmented Akt-mediated T cell differentiation. Consequently, Fas DNR–modified T cells retained a predominantly T_{CM}-like phenotype and the capacity to produce IL-2. In several different animal models (32, 61–64) and human clinical trials (11, 65), transfer of T_{CM}-like cells was associated with superior tumor regression compared with transfer of T_{EM}-like cells.

To control for the variable of T cell differentiation status, pmel-1 T cells transduced with $Fas^{\Delta DD}$ or an empty vector were enriched to greater than 97% purity for T_{CM}-like cells by FACS sorting for $Thy1.1^+CD44^{hi}CD62L^+$ cells immediately prior to cell infusion (Figure 5A). Purified T_{CM}-like cells were subsequently transferred into sublethally irradiated B6 mice bearing established B16 tumors. Treated mice also received IL-2 by i.p. injection. We found that adoptive transfer of tumor-specific T_{CM} cells modified with the Fas DNR resulted in superior tumor regression and animal survival compared with control-modified T cells (Figure 5, B and C; $P < 0.05$).

We next sought to extend our treatment findings using an independent tumor model in which a hematologic malignancy was targeted with a CAR. We utilized a recently developed syngeneic B cell ALL (B-ALL) line driven by the physiologically relevant E2a-PBX translocation in a treatment model using a murine second-generation 28ζ anti-CD19 CAR (57, 66). We specifically chose a syngeneic model over the more commonly used xenogeneic anti-CD19 CAR treatment models for two reasons. First, we wished to ensure that the transferred T cells were fully responsive to host-derived FasL in addition to FasL expression by tumor cells and the adoptively transferred T cells. Second, we wished to avoid the potentially confounding influence of xenogeneic reactivity on AICD induction in the transferred T cells.

We first established that dual transduction of B6 $CD8\alpha^+$ T cells with retroviral constructs containing the $Fas^{\Delta DD}$ or empty vector and anti-CD19 CAR was feasible (Figure 6, A and B). Using protein L to identify CAR-transduced T cells (67), we found that cotransduction efficiencies were similarly efficient using $Fas^{\Delta DD}$ and the empty vector control following Thy1.1 bead enrichment. Next, we measured how the cotransduced anti-CD19 CAR T cells responded to various apoptosis-inducing stimuli, including exogenous FasL, cytokine withdrawal, AICD, and exposure to antigen-expressing B-ALL tumor cells (Figure 6C). Similar to our results using TCR-expressing pmel-1 T cells, we found that the expression of $Fas^{\Delta DD}$ protected CAR-modified T cells from each of these death-inducing stimuli relative to empty vector control–transduced CAR^+ T cells.

We next tested whether coexpression of a Fas DNR in CAR-modified T cells resulted in higher persistence and superior antitumor efficacy in comparison to empty-transduced CAR-modified T cells, as observed in the pmel-1 TCR transgenic/B16 melanoma model. We infused $Fas^{\Delta DD}$ or empty $Thy1.1^+$ anti-CD19 CAR^+ $CD8\alpha^+$ T cells into sublethally irradiated B6 mice bearing 4-day-established E2a-PBX B-ALL (Figure 6D). Treated mice received daily IL-2 injections for 3 days to support expansion of the adoptively transferred T cells. Fourteen days following cell infusion, we analyzed the spleens and BM, two disease sites for E2a-PBX B-ALL, for persistence of the adoptively transferred cells. We measured higher levels of $Thy1.1^+$ $Fas^{\Delta DD}$ cells in both disease sites in comparison to mice that received empty vector–transduced T cells (Figure 6E). E2a-PBX leukemia expresses classic pre–B-ALL markers, including CD19, B220, and CD93 (66). As shown in Figure 6F, we found that the BM in untreated (PBS) and empty vector–treated mice contained roughly 70% leukemia cells 14 days after T cell treatment. However, the mice that received $Fas^{\Delta DD}$-modified cells contained less than 1% leukemia cells in the BM. These data indicated that CAR^+ T cells expressing the Fas DNR cells were able to mediate superior leukemia clearance relative to empty vector–transduced T cells.

Finally, we analyzed the survival of leukemia-bearing mice after adoptive transfer of two different doses of second-generation 28ζ anti-CD19 CAR–transduced T cells comodified with $Fas^{\Delta DD}$ or empty control. In order to provide for a treatment window, we intentionally transferred doses of CAR-modified T cells previously shown to be subtherapeutic in this model (57). At a higher cell dose (3×10^5 CAR^+ cells), we found that adoptive transfer of either control- or $Fas^{\Delta DD}$-modified CAR^+ T cells resulted in significantly improved animal survival compared with mice that did not receive treatment (Figure 6G, left). However, whereas all mice that received the Fas DNR–modified CAR^+ T cells survived, mice that received control-modified CAR^+ T cells did not survive longer than 55 days. At a further de-escalated dose of CAR^+ cells (2×10^5), Fas DNR-modified T cells continued to provide long-term survival in 100% of treated mice, while control-modified T cells entirely lost efficacy (Figure 6G, right). Previous reports have demonstrated that 4-1BB–containing second-generation CARs express higher

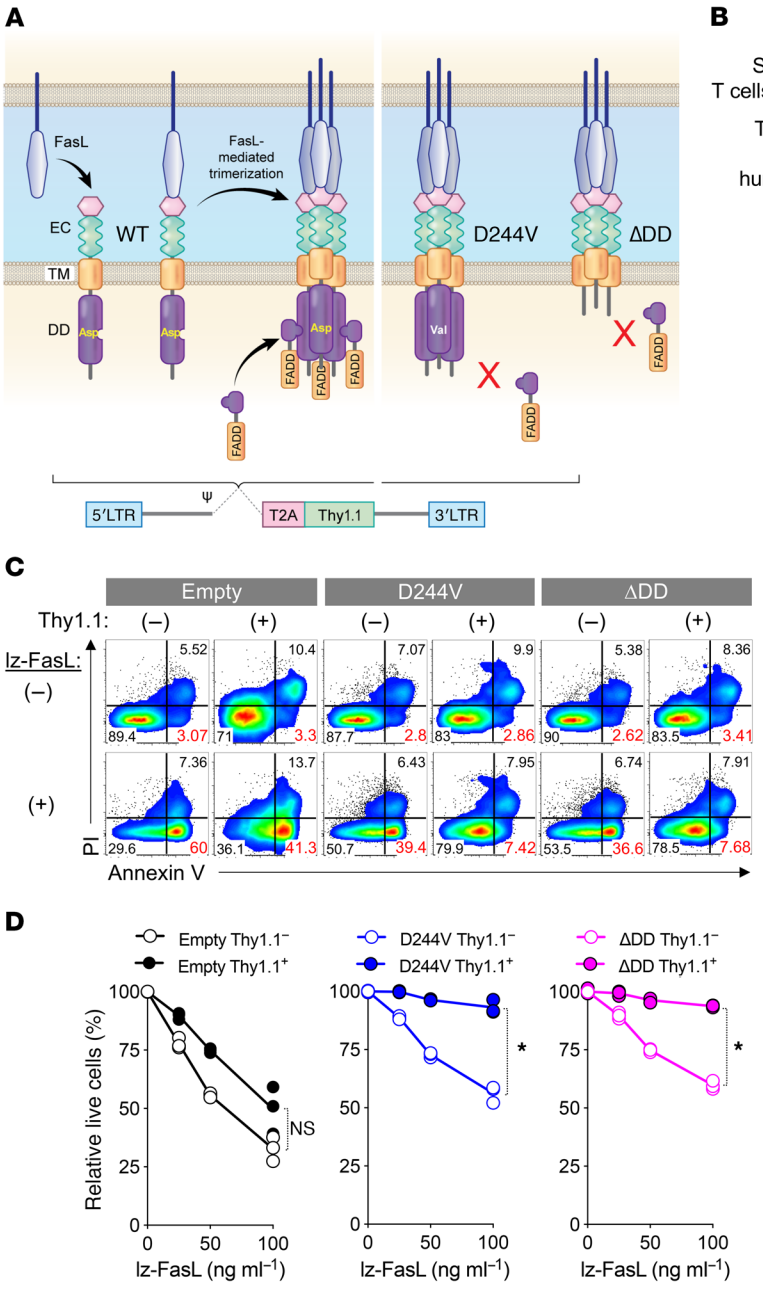

Figure 7. Genetic engineering with Fas DNR protects human T cells from FasL-induced apoptosis. (**A**) Schematic representation of physiologic Fas signaling and the design of 2 human Fas DNRs. Retrovirus-encoded human Fas DNRs were designed to prevent recruitment of FADD either by (i) substitution of a valine for an aspartic acid residue at position 244 of the DD ($hFas^{D244V}$) or (ii) truncation of the majority of the human intracellular DD ($hFas^{\Delta DD}$). An empty vector was used as a negative control. Receptors were cloned into a bicistronic vector containing a Thy1.1 reporter. (**B**) Experimental timeline for the stimulation, retroviral transduction, and testing of Iz-FasL–mediated apoptosis of human $CD8^+$ T cells modified with Fas^{D244V}, $Fas^{\Delta DD}$, or an empty vector control. (**C**) Representative FACS plots (0 and 100 ng ml^{-1} Iz-FasL) and (**D**) summary graph showing the frequency of live cells relative to the no Iz-FasL condition 6 hours following exposure to titrated concentrations of Iz-FasL. Results shown after gating on transduced ($Thy1.1^+$) or untransduced ($Thy1.1^-$) T cells. Data are displayed as mean ± SEM with $n = 3$ per condition and are representative of 3 independent experiments. $^*P < 0.05$, Wilcoxon's rank-sum test.

levels of antiapoptotic proteins compared with CARs containing a CD28 domain (68). We did not test in these experiments whether the Fas DNR could also enhance the function of a 4-1BB–containing CAR. Nevertheless, these data in the solid cancer B16 melanoma and hematologic E2a-PBX leukemia models indicate that Fas DNR expression in adoptively transferred T cells results in superior in vivo cellular persistence and antitumor efficacy regardless of whether the antigen-targeting structure is a TCR or 28ζ CAR.

Genetic engineering with Fas DNRs protects human T cells from Fas-mediated apoptosis. To determine the feasibility of engineering primary human T cells with Fas DNRs, we designed retroviral constructs encoding the human Fas sequence mutated to prevent FADD binding. This included a human Fas variant containing a point mutation substituting a valine for an aspartate residue at position 244 ($hFas^{D244V}$) (69, 70) and human Fas with the majority of the intracellular DD truncated (del aa230–314; $hFas^{\Delta DD}$) (Figure 7A) (69, 70). $CD8^+$ T cells were isolated from HD peripheral blood mononuclear cells (PBMCs) and stimulated with anti-CD3/CD28 and IL-2, followed by transduction with $hFas^{D244V}$, $hFas^{\Delta DD}$, or an empty vector control containing a Thy1.1 reporter (Figure 7B). In the absence of additional stimulation, untransduced $Thy1.1^-$ and transduced $Thy1.1^+$ T cells remained similarly viable, as measured by annexin V and PI staining (Figure 7C). However, when these cells were cultured in the presence of increasing doses of Iz-FasL, we found that T cells transduced with the empty vector exhibited a significant and dose-dependent increase in the frequency of annexin V^+ apoptotic and necrotic cells (Figure 7, C and D). By contrast, T cells modified with either $hFas^{D244V}$ or $hFas^{\Delta DD}$ were significantly protected from Iz-FasL–mediated apop-

tosis. Thus, we conclude that genetic engineering with a Fas DNR protects primary human T cells from FasL-induced cell death, providing a new method to potentially protect adoptively transferred T cells within the human TME.

Discussion

Herein, we report the results of a pan-cancer analysis that suggested that a canonical death-inducing ligand, *FASLG*, is overexpressed within the majority of human cancer microenvironments. We further discovered that a significant proportion of human T cells used for adoptive immunotherapy express Fas, the cognate receptor for FasL. Based on these findings, we developed a cell-intrinsic strategy to "insulate" Fas-competent mouse and human T cells from FasL-induced apoptosis using genetic engineering with a series of Fas DNRs. Functionally, adoptively transferred Fas DNR–modified T cells exhibited greater persistence in both the periphery and tumors of tumor-bearing animals, resulting in superior tumor regression and overall survival in both solid and liquid syngeneic cancer models. Importantly, while T cells modified with Fas DNR exhibited enhanced survival relative to control-modified T cells as late as 6 months following transfer, we detected no evidence of uncontrolled lymphoproliferation or autoimmunity. These findings therefore provide a potentially universal gene engineering strategy to enhance the function of adoptively transferred T cells against a broad range of human malignancies, including both solid and hematologic cancers.

We previously reported that in addition to its canonical apoptosis-inducing functions, Fas can also promote mouse and human T cell differentiation in an Akt-dependent manner (58, 59). Consistent with these findings, we discovered that T cells transduced with Fas DNRs were protected from lz-FasL–mediated induction of $pAkt^{S473}$ and $pS6^{S235,S236}$. Consequently, this block in Akt/mTOR signaling minimized T cell differentiation, promoting the accumulation of T_{CM}-like cells that retained expression of the lymphoid homing marker CD62L and the capacity to produce IL-2. In multiple preclinical models (32, 61, 62, 64) and in retrospective analyses of human clinical trials (11, 65), infusion of T_{CM}-like cells was associated with superior antitumor outcomes compared with T_{EM}-like cells. We therefore compared the antitumor efficacy of phenotypically matched, FACS-sorted T_{CM}-like cells modified with a Fas DNR or an empty vector control. We found that Fas DNR–modified T_{CM} cells exhibited superior treatment efficacy compared with control-modified T_{CM} cells. Mechanistically, we conclude that the dominant contributor of the enhanced in vivo antitumor efficacy we found using Fas DNR–modified T cells was attributable to the disruption of cell death and not the infusion of less-differentiated cells. These findings are also consistent with recent articles by Zhu et al., Horton et al., and Lakins et al. demonstrating that FasL-induced apoptosis of tumor-infiltrating lymphocytes limits the efficacy of immune checkpoint inhibitors (19, 71, 72).

While our analyses indicated that *FASLG* expression is enriched within the TMEs of many human tumors, they do not define which specific cell type is expressing the ligand. Using immunohistochemical protein staining, previous studies have demonstrated that FasL can be expressed directly on the surface of many of the solid cancers identified in our pan-cancer analysis. This includes cancers of the breast, colon, brain, kidney, and cervix (73, 74). Additionally, recent studies have also identified that FasL is expressed along the luminal surface of the neovasculature surrounding human ovarian and brain cancers, creating a tumor endothelial death barrier limiting T cell infiltration (73, 75). Further, it is possible that FasL can be expressed within the TME by cells of both the innate and adaptive immune system. This possibility has previously been shown by others (19) and is further suggested by our own analysis demonstrating a high degree of correlation between *FASLG* and many immune-related genes. Finally, our functional data demonstrate that Fas DNR modification also affords protection from other apoptosis-inducing stimuli a T cell might experience following adoptive cell transfer into a tumor-bearing host. These include AICD, cytokine withdrawal, and proximity to antigen-expressing tumor cells. Collectively, these data suggest that the Fas DNR can enhance T cell survival to a broad range of potential FasL sources, including tumor cells, nontransformed cells in the TME, as well as T cells themselves.

Fas DNR now joins a list of other candidate DNRs with which a T cell might be modified to intrinsically disrupt signaling by immune-suppressive factors present within the TME, including TGF-β (76) and PD1-L1/L2 (77). Disruption of Fas using a short hairpin RNA approach has been reported in human T cells in vitro (78); however, due to the relatively poor efficiency of Fas knockdown, this approach required lengthy in vitro selection. Furthermore, the in vivo antitumor capacity of these cells was not tested. Germline loss of function in Fas signaling can result in an autoimmune lymphoproliferative disease in both mice and humans, a potential safety consideration for the Fas DNR approach. Despite augmented survival of $Fas^{\Delta DD}$-modified T cells, we found no evidence of uncontrolled lymphoaccumulation, formation of an aberrant $CD3^+B220^+$ lymphocyte population, or autoimmunity using 2 different mouse strains. This included performing adoptive transfer of a polyclonal T cell population into the ALPS-prone MRL-Mp strain. Based on these data, we conclude that infusion of mature T cells impaired in Fas signaling is unlikely to result in an acquired lymphoproliferation syndrome.

Although Fas is a critical mediator for initiating the extrinsic apoptotic signaling cascade, intrinsic apoptotic pathways remain intact in our cells. Thus, competition for homeostatic cytokines, neglect due to an absence of antigen, and T cell exhaustion may all contribute to regulating the homeostasis of Fas DNR cells in vivo. Despite these reassuring safety data in mice, refinement of this approach for clinical application will include the introduction of a suicide mechanism, such as a truncated EGFR upstream of the Fas DNR (79, 80) or an inducible caspase-9 variant (81).

In conclusion, we have discovered that the FasL/Fas pathway is poised to be activated in many patients receiving adoptive immunotherapy for the treatment of human cancers. We have developed DNRs that intrinsically abrogate the apoptosis-inducing functions of this pathway in primary mouse and human T cells. This engineered resistance to Fas-mediated apoptosis in turn led to enhanced in vivo cellular persistence and augmented antitumor efficacy in 2 different syngeneic models for the treatment of a B16 melanoma and a B-ALL using TCR- and CAR-modified T cells, respectively. These data lay the groundwork for a potential universal strategy to enhance the potency of adoptive immunotherapies against both solid and hematologic cancers.

Methods

The Cancer Genome Atlas pan-cancer bioinformatics analysis. RNA-Seq data from 26 human cancers from the Cancer Genome Atlas (TCGA) data set and matched normal tissues from the GTEx data set were collected and analyzed by UCSC Xena (82) in the form of normalized RSEM values. *FASLG* gene expression as normalized RSEM counts was analyzed in each. Statistics were corrected by Mann-Whitney *U* test. To identify genes positively correlated to *FASLG* expression, we ran a pre-ranked gene set enrichment against all KEGG pathways in the Molecular Signatures (MSigDB) database. Pearson's correlation was performed on the top 1000 genes positively correlated to *FASLG* expression averaged across 26 TCGA histologies.

Human specimens. PBMCs were obtained from patients with melanoma and DLBCL enrolled in an adoptive immunotherapy clinical protocol, or from age- and sex-matched HDs.

Mice. Adult 6- to 12-week-old male or female B6 NCR (B6; Ly5.2$^+$) mice were purchased from Charles River Laboratories at NCI Frederick. B6.SJL-Ptprc^a Pepc^b/BoyJ (Ly5.1$^+$), B6.129S7-Rag1Lm/Mom/J(Rag), B6.MRL-Fas^{lpr}/J(B6-lpr), B6.Cg-Thy1^a/CyTg(TcraTcrb)8Rest/J (pmel-1; ref. 83)), MRL/MpJ (MRL-Mp), and MRL/MpJ-Fas^{lpr}/J (MRL-lpr) mice were purchased from the Jackson Laboratory. Where indicated, pmel-1 mice were crossed to a Ly5.1 or Rag background. All mice were maintained under specific pathogen–free conditions.

Retroviral vectors and transduction of murine and human CD8$^+$ T cells. Murine and human Fas cDNA sequences were synthesized and separately cloned (GenScript) into the MSGV retroviral plasmid preceding a T2A "self-cleavage" sequence and selectable marker Thy1.1. Murine T cell transductions were performed as previously described (84). Briefly, Platinum-E ecotropic packaging cells (Cell Biolabs Inc.) were plated on BioCoat 10cm dishes (Corning) overnight. The following day, 24 μg retroviral plasmid DNA encoding MSGV-Thy1.1 (empty), MSGV-WT-mFas-Thy1.1 (mWT), MSGV-I246N-mFas-Thy1.1 (Fas^{I246N}), MSGV-ΔDD-mFas-Thy1.1 (Fas$^{\Delta DD}$), or MSGV-1D3-28Z (anti-CD19 CAR) (55) was separately mixed with 6 μg pCL-Eco plasmid DNA along with 60 μl Lipofectamine 2000 (Thermo Fisher Scientific) in OptiMEM (Gibco), then applied to the Platinum-E cells for 7 hours in antibiotic-free 10% FBS–containing medium. Medium was replaced after 7 hours; viral supernatant was collected from the cells after 48 hours and centrifuged to remove debris. Retroviral supernatants were spun for 2 hours at 2000 *g*, 32°C on non–tissue culture–treated 24-well plates that had been coated overnight in 20 μg ml^{-1} Retronectin (Takara Bio Inc.). T cells activated for 24 hours were added to plates that had all but 100 μl viral supernatant removed, spun for 5 minutes at 300 *g* at 32°C, then incubated overnight. The transduction was performed a second time the next day. For human T cell transduction, 293T cells (ATCC) (85) and RD114 were used in place of Platinum-E cells and pCL-Eco, respectively, and proceeded as during the murine virus production described above.

T cell culture and Fas death assay. Human PBMCs from healthy donors or patients were obtained by either leukapheresis or venipuncture and centrifuged over a Ficoll-Hypaque (Lonza) gradient to remove red blood cells, then washed twice with PBS containing 1 mM EDTA, stained with fixable cell viability dye (Thermo Fisher Scientific) in PBS, then washed twice with PBS supplemented with 2% FBS and 1 mM EDTA (FACS buffer). Untouched human CD8α$^+$ T cells were isolated using a human CD8 isolation kit (STEMCELL Technologies). Murine and human T cells and E2a-PBX leukemia cells (57) were maintained in RPMI 1640 (Gibco) with 10% heat-inactivated FBS, 1% penicillin/streptomycin (100 U ml^{-1} and 100 μg ml^{-1}, respectively; Gibco), gentamicin (10 μg ml^{-1}, Gibco), MEM non-essential amino acids (Gibco), sodium pyruvate (1 nM, Gibco), GlutaMAX (2 mM, Gibco), 2-mercaptoethanol (0.011 mM, Gibco) and amphotericin B (250 ng ml^{-1}, Gibco). B16-mhgp100 tumor cells (a gift from K. Hanada, Surgery Branch, NCI), Platinum-E cells, and 293T cells were maintained in DMEM (Gibco) supplemented with 10% FBS and the above-mentioned additives.

Untouched murine CD8α$^+$ T cells were isolated from splenocytes using a MACS CD8$^+$ negative selection kit (Miltenyi Biotec) and stimulated in tissue culture–treated 24-well plates with plate-bound anti-CD3 (2 μg ml^{-1}, clone 145-2C11, BD Biosciences), soluble anti-CD28 (1 μg ml^{-1}, clone 37-51, BD Biosciences) and rhIL-2 (IL-2; 5 ng ml^{-1}, Prometheus). Pmel-1 T cells were stimulated in whole splenocyte cultures with 1 μg ml^{-1} human gp100$_{25–33}$ peptide and IL-2 (5 ng ml^{-1}). Human PBMCs or CD8α$^+$ T cells were stimulated with plate-bound anti-CD3 (1 μg ml^{-1}, clone OKT3, BD Biosciences) and soluble anti-CD28 (1 μg ml^{-1}, clone CD28.2, BD Biosciences) for 2 days, then treated with IL-2 (20 ng ml^{-1}) during the remainder of culture. Cells were stimulated for 24 hours before transduction with viral supernatant on days 1 and 2 of culture. On day 3 cells were removed from Retronectin-coated plates and returned to tissue culture–treated 24-well plates or flasks. Where noted cells were grown with either vehicle or the indicated concentrations of lz-FasL, a recombinant form of oligomerized FasL (45, 59). Five to 6 days (for murine cells) or 10–11 days (for human cells) after stimulation, T cells were washed twice, plated at 1×10^5 to 2×10^5 cells/well in a 96-well plate with the indicated concentrations of lz-FasL, and incubated at 37°C with 5% CO_2 for 6 or 24 hours. Cells were then washed twice and stained with either annexin V and PI or Live/Dead Fixable Dye (Thermo Fisher Scientific) as well as CD8α (clone 53-6.7, BD Biosciences) and Thy1.1 (clone HIS51, eBioscience).

Flow cytometry, intracellular cytokine staining, and phospho-flow. Cells were stained with fixable cell viability dye in PBS, then washed twice with FACS buffer. Human cells were stained with the following fluorochrome-conjugated antibodies: CD3 (UCHT1), CCR7 (3D12), CD45RA (HI100), CD45RO (UCHL1), CD28 (CD28.2), CD95 (DX2) (BD Biosciences); and CD27 (M-T271), CD62L (DREG-56), CD8α (SK1), CD4 (OKT4) (BioLegend). Murine T cells, BM, and splenocytes were stained with the following antibodies: CD3 (clone 145-2C11), CD8α (clone 53-6.7), Vβ13 (MR12-3), Ly5.1 (A20), Ly5.2 (clone 104), CD62L (MEL-14), CD95 (Jo2), B220 (RA3-6B2) (BD Biosciences); CD44 (IM7), CD19 (6D5), CD93 (AA4.1) (BioLegend); Thy1.1 (HIS51, eBioscience). For anti-CD19 CAR detection (67) Biotin-Protein L (GenScript) was utilized.

For phospho-flow, cells were fixed and permeabilized using the BD Biosciences Phosflow reagents and following the manufacturer's protocol. After permeabilization, cells were stained with pAkt (S473) (D9E) and pS6 (S235/236) (D57.2.2E) from Cell Signaling Technology. For intracellular cytokine staining, cells were stained for surface antibodies in FACS buffer, then fixed and permeabilized (BD Biosciences) and stained for IFN-γ (XMG1.2, BD Biosciences) and IL-2 (JES6-5H4, BioLegend). For FasL staining, tumor cells were incubated with vehicle (PBS) or murine IFN-γ (100 ng ml^{-1}, BioLegend) for 24 hours, then stained with FasL (Kay-10) and H-2Db

(KH95) (BD Biosciences). All flow cytometric data were acquired using a BD Fortessa flow cytometer (BD Biosciences) and analyzed using FlowJo v. 9.9 software (Tree Star).

Sanger sequencing analysis. Genomic DNA from Thy1.1-enriched empty vector– or Fas^{I246N}-transduced cells was extracted using the AllPrep DNR/RNA Mini Kit (QIAGEN). Primers (IDT) were designed such that the forward primer was located in Fas upstream of the Fas^{I246N} point mutation and the reverse primer in the Thy1.1 reporter. After PCR amplification (Invitrogen) Sanger sequencing was performed by the NCI Sequencing Core Facility.

ACT, T cell enumeration, and tumor treatment. For analysis of in vivo persistence, male or female B6 mice aged 6–12 weeks received 6 Gy total body irradiation. One day later, they were injected by tail vein injection with 5×10^5 congenically marked pmel-1 T cells transduced with a Thy1.1-containing reporter construct. Mice were sacrificed on the indicated days, and splenocytes were analyzed for homeostatic expansion of pmel-1 T cells.

For tumor treatment experiments, male or female B6 mice aged 6–12 weeks were injected with 5×10^5 cells of a previously described B16 melanoma line (86) that overexpresses the chimeric human/mouse gp100 antigen KVPRNQDWL (aa25–33) or 1×10^6 $CD19^+$ E2a-PBX leukemia cells. Tumor-bearing mice received 5–6 Gy total body irradiation on the indicated days. Mice were left untreated as controls or received by tail vein injection the indicated doses of congenically marked pmel-1 or anti-CD19 CAR–transduced T cells modified with a Thy1.1-containing reporter construct. To analyze anti-CD19 CAR–transduced T cell persistence and leukemia burden, we sacrificed mice after 14 days and performed cellular analysis on the spleen and BM.

For experiments with MRL-Mp mice, female mice aged 8 weeks received 6 Gy total body irradiation. One day later, mice were injected with 3×10^6 anti-CD19 CAR–transduced $CD8\alpha^+$ T cells also transduced with a Thy1.1-containing reporter construct. Age-matched MRL-lpr female mice were left unmanipulated as an ALPS positive control.

All transduced T cells were bead-enriched to >92% purity using anti-Thy1.1 magnetic microbeads prior to infusion (Miltenyi Biotec). All treated mice received once-daily injections of 12 μg IL-2 i.p. for 3 days. All tumor measurements were performed in a blinded fashion by an independent investigator.

T cell and tumor cell coculture assay. After 5–6 days in culture, T cells were washed twice in PBS and plated in IL-2–free T cell media at 5×10^4 cells per well in a 96-well round-bottom plate. T cells were incubated either alone, with plate-bound anti-CD3/CD28 (2 μg ml^{-1}, each), with 1.5×10^5 B16-mhgp100 or E2a-PBX cells per well for an E/T of 1:3, or with 50–100 ng ml^{-1} lz-FasL. Cells were cultured together for 6 or 24 hours before being washed and stained for cell viability.

ELISA assay. Analysis of serum anti-nuclear and anti-dsDNA antibodies was performed on serum diluted 1:5; ELISA was performed according to the manufacturer's instructions (Alpha Diagnostic International).

Histopathology. Lung tissues were fixed in buffered 10% formalin and stained with H&E. Tissue sections were scored in a blinded manner by an interpreting pathologist. Scoring was as follows: 0, no specific findings; 1, mild infiltrates; 2, minimal infiltrates; 3, moderate infiltrates; 4, severe infiltrates.

Statistics. The products of perpendicular tumor diameters were plotted as the mean ± SEM for each data point; tumor treatment graphs were compared using Wilcoxon's rank-sum test, and analysis of animal survival was assessed using log-rank Mantel-Cox test. For all other experiments, data were compared using either unpaired 2-tailed Student's *t* test corrected for multiple comparisons by Bonferroni's adjustment or repeated measures using 1- or 2-way ANOVA, as indicated. In all cases, *P* values less than 0.05 were considered significant. Statistics were calculated using GraphPad Prism 7 software.

Study approval. All anonymous NIH Blood Bank donors and cancer patients providing PBMC samples were enrolled in clinical trials approved by the NIH Clinical Center and NCI institutional review boards. Each patient signed an informed consent form and received a patient information form prior to participation. Animal experiments were approved by the Institutional Animal Care and Use Committees of the NCI and performed in accordance with NIH guidelines.

Data and materials availability. All data reported herein are recorded in the manuscript, or are available in the supplemental materials or through the publicly available databases TCGA (https://cancergenome.nih.gov/) and UCSC Xena (http://xena.ucsc.edu).

Author contributions

TNY, NPR, and CAK designed and conceived of all experiments and wrote and edited the manuscript. TNY and PHL performed all tissue culture, retroviral transduction, and immune-phenotyping experiments. SKV, DG, and RJK assisted in RNA-Seq analysis and experimental design. RE assisted in the design and generation of Fas DNR–engineered T cells. JF and LG assisted in experimental design and performing in vivo experiments. JNK and TJF provided in vivo reagents and helpful discussion on performing in vivo experiments. TNY, ZY, and AE performed in vivo experiments and all animal husbandry and colony management. ACC and RMS provided the lz-FasL reagent and assisted with death assays and experimental design. BAA and JEH assisted with all bioinformatic analyses. All coauthors edited and commented on the final manuscript.

Acknowledgments

We thank K. Hanada for contributing the B16-mhgp100 melanoma cell line. We thank S. Patel, S.M. Sukumar, and C. Ouyang for thoughtful discussions; R. Somerville for assistance with patient sample collection; A. Mixon and S. Farid for expertise with cell sorting; B. Karim for histopathology analysis and helpful discussions; and M. Cam and A. Merchant for help with bioinformatics analysis. This work was funded by the National Cancer Institute, Center for Cancer Research (NPR and CAK). Additional funding was provided to CAK by the Parker Institute for Cancer Immunotherapy, Damon Runyon Cancer Research Foundation, William H. Goodwin and Alice Goodwin and the Commonwealth Foundation for Cancer Research, Center for Experimental Therapeutics at MSKCC, and MSKCC Core grant P30 CA008748.

Address correspondence to: Christopher A. Klebanoff, Memorial Sloan Kettering Cancer Center, 300 East 60th Street, Office #747, New York, New York 10065, USA. Phone: 646.888.4572; Email: klebanoc@mskcc.org.

RMS's present address is: Novartis Institutes for BioMedical Research, Basel, Switzerland.

1. Maude SL, et al. Tisagenlecleucel in children and young adults with B-cell lymphoblastic leukemia. *N Engl J Med*. 2018;378(5):439–448.
2. Neelapu SS, et al. Axicabtagene ciloleucel CAR T-cell therapy in refractory large B-cell lymphoma. *N Engl J Med*. 2017;377(26):2531–2544.
3. Schuster SJ, et al. Chimeric antigen receptor T cells in refractory B-cell lymphomas. *N Engl J Med*. 2017;377(26):2545–2554.
4. Lee DW, et al. T cells expressing CD19 chimeric antigen receptors for acute lymphoblastic leukaemia in children and young adults: a phase 1 dose-escalation trial. *Lancet*. 2015;385(9967):517–528.
5. Porter DL, et al. Chimeric antigen receptor T cells persist and induce sustained remissions in relapsed refractory chronic lymphocytic leukemia. *Sci Transl Med*. 2015;7(303):303ra139.
6. Turtle CJ, et al. Immunotherapy of non-Hodgkin's lymphoma with a defined ratio of CD8+ and CD4+ CD19-specific chimeric antigen receptor-modified T cells. *Sci Transl Med*. 2016;8(355):355ra116.
7. Ramos CA, et al. Clinical and immunological responses after CD30-specific chimeric antigen receptor-redirected lymphocytes. *J Clin Invest*. 2017;127(9):3462–3471.
8. Park JH, et al. Long-term follow-up of CD19 CAR therapy in acute lymphoblastic leukemia. *N Engl J Med*. 2018;378(5):449–459.
9. Fry TJ, et al. CD22-targeted CAR T cells induce remission in B-ALL that is naive or resistant to CD19-targeted CAR immunotherapy. *Nat Med*. 2018;24(1):20–28.
10. Siegel RL, Miller KD, Jemal A. Cancer statistics, 2018. *CA Cancer J Clin*. 2018;68(1):7–30.
11. Louis CU, et al. Antitumor activity and long-term fate of chimeric antigen receptor-positive T cells in patients with neuroblastoma. *Blood*. 2011;118(23):6050–6056.
12. Parkhurst MR, et al. T cells targeting carcinoembryonic antigen can mediate regression of metastatic colorectal cancer but induce severe transient colitis. *Mol Ther*. 2011;19(3):620–626.
13. Ahmed N, et al. Human epidermal growth factor receptor 2 (HER2) -specific chimeric antigen receptor-modified T cells for the immunotherapy of HER2-positive sarcoma. *J Clin Oncol*. 2015;33(15):1688–1696.
14. Lu YC, et al. Treatment of patients with metastatic cancer using a major histocompatibility complex class II-restricted T-cell receptor targeting the cancer germline antigen MAGE-A3. *J Clin Oncol*. 2017;35(29):3322–3329.
15. Veatch JR, et al. Tumor-infiltrating BRAFV600E-specific CD4+ T cells correlated with complete clinical response in melanoma. *J Clin Invest*. 2018;128(4):1563–1568.
16. Klebanoff CA, Rosenberg SA, Restifo NP. Prospects for gene-engineered T cell immunotherapy for solid cancers. *Nat Med*. 2016;22(1):26–36.
17. Maus MV, June CH. Making better chimeric antigen receptors for adoptive T-cell therapy. *Clin Cancer Res*. 2016;22(8):1875–1884.
18. Gattinoni L, Klebanoff CA, Restifo NP. Paths to stemness: building the ultimate antitumour T cell. *Nat Rev Cancer*. 2012;12(10):671–684.
19. Zhu J, et al. Resistance to cancer immunotherapy mediated by apoptosis of tumor-infiltrating lymphocytes. *Nat Commun*. 2017;8(1):1404.
20. Rosenberg SA, et al. Durable complete responses in heavily pretreated patients with metastatic melanoma using T-cell transfer immunotherapy. *Clin Cancer Res*. 2011;17(13):4550–4557.
21. Stevanović S, et al. Landscape of immunogenic tumor antigens in successful immunotherapy of virally induced epithelial cancer. *Science*. 2017;356(6334):200–205.
22. D'Angelo SP, et al. Antitumor activity associated with prolonged persistence of adoptively transferred NY-ESO-1 ^{c259}T cells in synovial sarcoma. *Cancer Discov*. 2018;8(8):944–957.
23. Heczey A, et al. CAR T cells administered in combination with lymphodepletion and PD-1 inhibition to patients with neuroblastoma. *Mol Ther*. 2017;25(9):2214–2224.
24. Chong EA, et al. PD-1 blockade modulates chimeric antigen receptor (CAR)-modified T cells: refueling the CAR. *Blood*. 2017;129(8):1039–1041.
25. Adams GP, et al. High affinity restricts the localization and tumor penetration of single-chain fv antibody molecules. *Cancer Res*. 2001;61(12):4750–4755.
26. Postow MA, Sidlow R, Hellmann MD. Immune-related adverse events associated with immune checkpoint blockade. *N Engl J Med*. 2018;378(2):158–168.
27. Aran D, et al. Comprehensive analysis of normal adjacent to tumor transcriptomes. *Nat Commun*. 2017;8(1):1077.
28. Consortium GT. The Genotype-Tissue Expression (GTEx) project. *Nat Genet*. 2013;45(6):580–585.
29. Li B, Dewey CN. RSEM: accurate transcript quantification from RNA-Seq data with or without a reference genome. *BMC Bioinformatics*. 2011;12:323.
30. Subramanian A, et al. Gene set enrichment analysis: a knowledge-based approach for interpreting genome-wide expression profiles. *Proc Natl Acad Sci U S A*. 2005;102(43):15545–15550.
31. Hamann D, et al. Phenotypic and functional separation of memory and effector human CD8+ T cells. *J Exp Med*. 1997;186(9):1407–1418.
32. Gattinoni L, et al. A human memory T cell subset with stem cell-like properties. *Nat Med*. 2011;17(10):1290–1297.
33. Pauken KE, et al. Epigenetic stability of exhausted T cells limits durability of reinvigoration by PD-1 blockade. *Science*. 2016;354(6316):1160–1165.
34. Mackall CL, et al. Distinctions between CD8+ and CD4+ T-cell regenerative pathways result in prolonged T-cell subset imbalance after intensive chemotherapy. *Blood*. 1997;89(10):3700–3707.
35. Kägi D, et al. Fas and perforin pathways as major mechanisms of T cell-mediated cytotoxicity. *Science*. 1994;265(5171):528–530.
36. Hao Z, Hampel B, Yagita H, Rajewsky K. T cell-specific ablation of Fas leads to Fas ligand-mediated lymphocyte depletion and inflammatory pulmonary fibrosis. *J Exp Med*. 2004;199(10):1355–1365.
37. Mohamood AS, et al. Protection from autoimmune diabetes and T-cell lymphoproliferation induced by FasL mutation are differentially regulated and can be uncoupled pharmacologically. *Am J Pathol*. 2007;171(1):97–106.
38. Siegel RM, et al. Fas preassociation required for apoptosis signaling and dominant inhibition by pathogenic mutations. *Science*. 2000;288(5475):2354–2357.
39. Boldin MP, Varfolomeev EE, Pancer Z, Mett IL, Camonis JH, Wallach D. A novel protein that interacts with the death domain of Fas/APO1 contains a sequence motif related to the death domain. *J Biol Chem*. 1995;270(14):7795–7798.
40. Chinnaiyan AM, O'Rourke K, Tewari M, Dixit VM. FADD, a novel death domain-containing protein, interacts with the death domain of Fas and initiates apoptosis. *Cell*. 1995;81(4):505–512.
41. Medema JP, et al. FLICE is activated by association with the CD95 death-inducing signaling complex (DISC). *EMBO J*. 1997;16(10):2794–2804.
42. Kischkel FC, et al. Cytotoxicity-dependent APO-1 (Fas/CD95)-associated proteins form a death-inducing signaling complex (DISC) with the receptor. *EMBO J*. 1995;14(22):5579–5588.
43. June CH, Blazar BR, Riley JL. Engineering lymphocyte subsets: tools, trials and tribulations. *Nat Rev Immunol*. 2009;9(10):704–716.
44. Watanabe-Fukunaga R, Brannan CI, Copeland NG, Jenkins NA, Nagata S. Lymphoproliferation disorder in mice explained by defects in Fas antigen that mediates apoptosis. *Nature*. 1992;356(6367):314–317.
45. Ramaswamy M, et al. Specific elimination of effector memory CD4+ T cells due to enhanced Fas signaling complex formation and association with lipid raft microdomains. *Cell Death Differ*. 2011;18(4):712–720.
46. Imtiyaz HZ, Zhang Y, Zhang J. Structural requirements for signal-induced target binding of FADD determined by functional reconstitution of FADD deficiency. *J Biol Chem*. 2005;280(36):31360–31367.
47. Chandran SS, et al. Treatment of metastatic uveal melanoma with adoptive transfer of tumour-infiltrating lymphocytes: a single-centre, two-stage, single-arm, phase 2 study. *Lancet Oncol*. 2017;18(6):792–802.
48. Chapuis AG, et al. T-cell therapy using interleukin-21-primed cytotoxic T-cell lymphocytes combined with cytotoxic T-cell lymphocyte antigen-4 blockade results in long-term cell persistence and durable tumor regression. *J Clin Oncol*. 2016;34(31):3787–3795.
49. Cohen PL, Eisenberg RA. Lpr and gld: single gene models of systemic autoimmunity and lymphoproliferative disease. *Annu Rev Immunol*. 1991;9:243–269.
50. Rao VK, Oliveira JB. How I treat autoimmune lymphoproliferative syndrome. *Blood*. 2011;118(22):5741–5751.
51. Morse HC, Davidson WF, Yetter RA, Murphy ED, Roths JB, Coffman RL. Abnormalities induced by the mutant gene Ipr: expansion of a unique lymphocyte subset. *J Immunol*. 1982;129(6):2612–2615.
52. Izui S, Kelley VE, Masuda K, Yoshida H, Roths JB, Murphy ED. Induction of various autoantibodies by mutant gene lpr in several strains of mice. *J Immunol*. 1984;133(1):227–233.
53. Mountz JD, Bluethmann H, Zhou T, Wu J. Defective clonal deletion and anergy induction in TCR transgenic lpr/lpr mice. *Semin Immunol*.

1994;6(1):27–37.
54. Singer GG, Carrera AC, Marshak-Rothstein A, Martínez C, Abbas AK. Apoptosis, Fas and systemic autoimmunity: the MRL-lpr/lpr model. *Curr Opin Immunol*. 1994;6(6):913–920.
55. Kochenderfer JN, Yu Z, Frasheri D, Restifo NP, Rosenberg SA. Adoptive transfer of syngeneic T cells transduced with a chimeric antigen receptor that recognizes murine CD19 can eradicate lymphoma and normal B cells. *Blood*. 2010;116(19):3875–3886.
56. Slaney CY, et al. Dual-specific chimeric antigen receptor T cells and an indirect vaccine eradicate a variety of large solid tumors in an immunocompetent, self-antigen setting. *Clin Cancer Res*. 2017;23(10):2478–2490.
57. Yang Y, et al. TCR engagement negatively affects CD8 but not CD4 CAR T cell expansion and leukemic clearance. *Sci Transl Med*. 2017;9(417):eaag1209.
58. Klebanoff CA, et al. Memory T cell-driven differentiation of naive cells impairs adoptive immunotherapy. *J Clin Invest*. 2016;126(1):318–334.
59. Cruz AC, et al. Fas/CD95 prevents autoimmunity independently of lipid raft localization and efficient apoptosis induction. *Nat Commun*. 2016;7:13895.
60. Yi F, Frazzette N, Cruz AC, Klebanoff CA, Siegel RM. Beyond cell death: new functions for TNF family cytokines in autoimmunity and tumor immunotherapy. *Trends Mol Med*. 2018;24(7):642–653.
61. Klebanoff CA, et al. Central memory self/tumor-reactive CD8+ T cells confer superior antitumor immunity compared with effector memory T cells. *Proc Natl Acad Sci U S A*. 2005;102(27):9571–9576.
62. Sommermeyer D, et al. Chimeric antigen receptor-modified T cells derived from defined CD8+ and CD4+ subsets confer superior antitumor reactivity in vivo. *Leukemia*. 2016;30(2):492–500.
63. Klebanoff CA, et al. Determinants of successful CD8+ T-cell adoptive immunotherapy for large established tumors in mice. *Clin Cancer Res*. 2011;17(16):5343–5352.
64. Klebanoff CA, et al. Inhibition of AKT signaling uncouples T cell differentiation from expansion for receptor-engineered adoptive immunotherapy. *JCI Insight*. 2017;2(23):95103.
65. Kochenderfer JN, et al. Lymphoma remissions caused by anti-CD19 chimeric antigen receptor T cells are associated with high serum interleukin-15 levels. *J Clin Oncol*. 2017;35(16):1803–1813.
66. Jacoby E, Yang Y, Qin H, Chien CD, Kochenderfer JN, Fry TJ. Murine allogeneic CD19 CAR T cells harbor potent antileukemic activity but have the potential to mediate lethal GVHD. *Blood*. 2016;127(10):1361–1370.
67. Zheng Z, Chinnasamy N, Morgan RA. Protein L: a novel reagent for the detection of chimeric antigen receptor (CAR) expression by flow cytometry. *J Transl Med*. 2012;10:29.
68. Li G, et al. 4-1BB enhancement of CAR T function requires NF-κB and TRAFs. *JCI Insight*. 2018;3(18):121322.
69. Martin DA, et al. Defective CD95/APO-1/Fas signal complex formation in the human autoimmune lymphoproliferative syndrome, type Ia. *Proc Natl Acad Sci U S A*. 1999;96(8):4552–4557.
70. Jackson CE, et al. Autoimmune lymphoproliferative syndrome with defective Fas: genotype influences penetrance. *Am J Hum Genet*. 1999;64(4):1002–1014.
71. Horton BL, Williams JB, Cabanov A, Spranger S, Gajewski TF. Intratumoral CD8+ T-cell apoptosis is a major component of T-cell dysfunction and impedes antitumor immunity. *Cancer Immunol Res*. 2018;6(1):14–24.
72. Lakins MA, Ghorani E, Munir H, Martins CP, Shields JD. Cancer-associated fibroblasts induce antigen-specific deletion of CD8 + T Cells to protect tumour cells. *Nat Commun*. 2018;9(1):948.
73. Kleber S, et al. Yes and PI3K bind CD95 to signal invasion of glioblastoma. *Cancer Cell*. 2008;13(3):235–248.
74. Peter ME, et al. The role of CD95 and CD95 ligand in cancer. *Cell Death Differ*. 2015;22(4):549–559.
75. Motz GT, et al. Tumor endothelium FasL establishes a selective immune barrier promoting tolerance in tumors. *Nat Med*. 2014;20(6):607–615.
76. Bollard CM, et al. Tumor-specific T-cells engineered to overcome tumor immune evasion induce clinical responses in patients with relapsed hodgkin lymphoma. *J Clin Oncol*. 2018;36(11):1128–1139.
77. Cherkassky L, et al. Human CAR T cells with cell-intrinsic PD-1 checkpoint blockade resist tumor-mediated inhibition. *J Clin Invest*. 2016;126(8):3130–3144.
78. Dotti G, et al. Human cytotoxic T lymphocytes with reduced sensitivity to Fas-induced apoptosis. *Blood*. 2005;105(12):4677–4684.
79. Wang X, et al. A transgene-encoded cell surface polypeptide for selection, in vivo tracking, and ablation of engineered cells. *Blood*. 2011;118(5):1255–1263.
80. Paszkiewicz PJ, et al. Targeted antibody-mediated depletion of murine CD19 CAR T cells permanently reverses B cell aplasia. *J Clin Invest*. 2016;126(11):4262–4272.
81. Straathof KC, et al. An inducible caspase 9 safety switch for T-cell therapy. *Blood*. 2005;105(11):4247–4254.
82. Goldman M, Craft B, Zhu JC, Haussler D. The UCSC Xena system for cancer genomics data visualization and interpretation. *Cancer Res*. 2017;77(13 suppl):2584.
83. Overwijk WW, et al. Tumor regression and autoimmunity after reversal of a functionally tolerant state of self-reactive CD8+ T cells. *J Exp Med*. 2003;198(4):569–580.
84. Kerkar SP, et al. Genetic engineering of murine CD8+ and CD4+ T cells for preclinical adoptive immunotherapy studies. *J Immunother*. 2011;34(4):343–352.
85. Robbins PF, et al. Tumor regression in patients with metastatic synovial cell sarcoma and melanoma using genetically engineered lymphocytes reactive with NY-ESO-1. *J Clin Oncol*. 2011;29(7):917–924.
86. Eil R, et al. Ionic immune suppression within the tumour microenvironment limits T cell effector function. *Nature*. 2016;537(7621):539–543.